Lab on a Chip

Accepted Manuscript

ROYAL SOCIETY OF CHEMISTRY

www.rsc.org/loc

Label-free whole blood cell differentiation based on multiple frequency AC impedance and light scatter analysis in a micro flow cytometer

Peter Simon*, Marcin Frankowski*, Nicole Bock, Jörg Neukammer

Physikalisch-Technische Bundesanstalt (PTB), Abbestrasse 2-12, 10587 Berlin, Germany

Keywords: label-free cell differentiation; whole blood analysis; micro fabricated flow cytometer; single cell analysis; immunofluorescence; impedance flow cytometry; complete blood count

* Both authors contributed equally to this work

Abstract

We developed a microfluidic sensor for label-free flow cytometric cell differentiation by combined multiple AC electrical impedance and light scattering analysis. The measured signals are correlated to cell volume, membrane capacity and optical properties of single cells. For improved signal to noise ratio the microfluidic sensor incorporates two electrode pairs for differential impedance detection. A one-dimensional sheath flow focusing was implemented, which allows single particle analysis at kHz count rates. Various monodisperse particles and differentiation of leukocytes in haemolysed samples served to benchmark the microdevice applying combined AC impedance and side scatter analyses. As follows, we demonstrate that AC impedance measurements at selected frequencies allow label-free discrimination of platelets, erythrocytes, monocytes, granulocytes and lymphocytes in whole blood samples involving dilution only. Immunofluorescence staining was applied to validate the results of the label-free cell analysis. Reliable differentiation and enumeration of cells in whole blood by AC impedance detection has the potential to support medical diagnosis for patients with haemolysis resistant erythrocytes or abnormally sensitive leucocytes, i.e. for patient suffering from anaemia or leukaemia.

Introduction

Medical decision making frequently relies on the blood cell count as a fast accessible routine diagnostic method for many diseases. Fast and accurate single cell detection requires technological solutions for sample preparation, handling and reliable classification of cells. Because of the broad range of applications, which covers haematology, immunology, oncology and characterisation of blood products, a variety of instruments and measurement procedures are presently available [1], [2], [3]. In our experiments, we developed a micro flow cytometric sensor and differentiated erythrocytes, platelets, lymphocytes, monocytes and granulocytes in diluted whole blood samples by alternate-current (AC) impedance measurements. We demonstrated label-free differentiation of single cells based on complex impedance measurement at two frequencies. The advantage of this method is that sample preparation, which might e.g. destroy abnormally sensitive white blood cells in leukaemia patients during haemolysis, is avoided.

The first approach for cell counting in flow at kHz rates was established in the 1950s, based on direct-current (DC) impedance change detection when a particle passes a small orifice, the well known Coulter principle [4], [5]. Particle differentiation relies on the discrimination of their respective volumes. AC impedance measurements, also referred to as capacitance method, were introduced in the late 1970s [6], [7]. Whereas DC impedance signals depend on the volume of a cell, AC impedance gives additional information about membrane capacity and resistance, cytoplasm conductivity and permittivity [8], [9]. At present, two groups of instruments are routinely applied for cell counting in haematology laboratories. Optical flow cytometers or haematology analysers use light scatter and fluorescence measurements for cell identification [10], [11], [12]. Fluorescence based instruments for counting stained cells were developed and introduced in 1969 [13]. Multi colour fluorescence detection allows immunological cell differentiation employing specific antibodies labelled with fluorescent dye. Such procedure is capable to distinguish morphologically identical cells like lymphocyte subpopulations and to classify them according to their biological function. In the second group of devices combinations of DC / AC impedance and optical methods are integrated and hence designated as hybrid counters [14], [15].

In haematology, most frequently the measurands of the complete blood count (CBC), i.e. the concentrations of erythrocytes (RBC), platelets (Plt) and leucocytes (WBC) are determined. Generally, the CBC is supplemented by the differentiation of white blood cells (WBC) in 3 subpopulations (WBC 3-part differential), i.e. lymphocytes (Ly), monocytes (M) and granulocytes (G), or in 5 subpopulations (WBC 5-part differential) by further distinguishing the granulocytes in neutrophils (G_n), eosinophils (G_e) and basophils (G_b). Different protocols for the determination of the CBC by haematology analysers are reviewed in [16]. Generally, two different preparations are required for the CBC in routine haematology analysers. While RBC and Plt are measured in the same diluted whole blood sample applying the DC impedance method or light scatter measurements, for the determination of WBC concentrations red blood cells are destroyed by haemolysis. These protocols are known to provide unreliable results for WBC counting in patients with sickle cell anaemia and in newborns, since the red blood cells are resistant to haemolysis and thus false high values for WBC are reported [14], [17], [18]. For such samples, label-free whole blood analysis as described in our paper or an alternative optical approach [19] would result in a significant improvement of the results on white blood cell concentrations and cost intensive microscopic differentiation as follow up analysis can be circumvented.

Apart from the general flow cytometric approach in routine application, i.e. to destroy RBC by haemolysis to determine WBC concentrations, various methods like mechanical or

hydrodynamic filtration are being investigated, which enable differentiation between RBC and WBC populations without the need of destroying red blood cells by a haemolysis treatment [20], [21], [22], [23]. Li et al. [20] separated the WBC population using microfiltration membranes in a microfluidic device. With a sample throughput of 1mL h^{-1} the device allowed a very fast cell separation for unprocessed whole blood. Since only 27.4 % of the WBC could be recovered, relative concentration measurements are difficult. Davis et al. [21] used arrays of microposts for physical cell separation and achieved much higher recovery rates for the WBC population. However, a cross contamination by red blood cells was evident and no further differentiation of the WBC subpopulations was possible by this technique. These methods are ideally suited for cell enrichment, but in general prevent a precise blood count if used as a pre-stage to replace haemolysis treatment.

Label-free cell differentiation in microflow cytometers including haemolysis treatment was discussed by comparing AC impedance phase and magnitude. Discrimination of subpopulations of human leukocytes according to the WBC 3-part differential was demonstrated by Holmes et al. [24] and Spencer et al. [25] for blood haemolysed in bulk. Berkel et al. [26] differentiated platelets and erythrocytes in whole blood and leukocyte subpopulations in blood, which was haemolysed in a microfluidic network with integrated sample preparation. Determination of their relative concentrations was compared for the microfluidic structures and a routine full blood counter. The AC frequencies chosen did not allow the differentiation of the three WBC subpopulations applying standard soft haemolysis protocols which approximately conserve the cell morphology. However, by applying saponin for haemolysis, the WBC 3-part differential was successfully measured and a good agreement for the relative concentrations derived from the microfluidic cytometer and the routine blood cell counter was observed. Nguyen et al. [27] combined on-chip sample preparation including RBC haemolysis treatment and RBC dilution with electrical measurements for analysing RBC and WBC parameters on the same device. Gawad et al. [28] reported label-free identification of intact erythrocytes and erythrocyte ghosts, which lost their haemoglobin and thus behave like vesicles. Besides haematology, recent reports indicate that label-free impedance microflow cytometry can be potentially applied to discriminate MCF-7 breast cancer cells and to assess their viability [29] [30]. Impedance cytometry is also used for non-invasive study of calcium-entry pathway as a measure of proliferative capacity of cells [31]. Pierzchalski et al. [32] assessed the viability of hybridoma cells and correlated the impedance analysis with fluorescence-based determination. Comprehensive reviews on microfluidic impedance cytometry were given by Chen et al. [33], Sun and Morgan [34], Cheung et al. [35] and Zheng et al. [36]. A topical overview on microfluidics in medical applications and a detailed introduction to impedance cytometry for blood cell analysis by H. Morgan and D. Spencer [37] is given in reference [38].

Supplementary to conventional manufacturing approaches, microtechnology facilitates the development of complex and highly integrated system components for combined electrical and optical particle detection. Reduced sensing volumes compared to conventional solutions applied in coulter-counter devices allow improving measurement sensitivity. It further offers the advantage to implement reference electrodes for differential detection which increases the signal stability. High throughput single cell analyses demand stable particle positioning in a flow channel, which is a challenging task in microfluidic devices. This has been accomplished through various techniques like AC dielectrophoretic (DEP) [8], [39] and acoustic focusing [40], [41] or sheath-flow [42], [43], [44] and sheath-less hydrodynamic focusing [25]. Particular techniques are thoroughly reviewed in literature [45].

In this article, we demonstrate the performance of a microfabricated AC impedance cytometer for blood cell differentiation. The estimated limit of detection (LOD) for particle volumes using threshold based analyses is about 2 fL, corresponding to a diameter of 1.5 µm. This allows discrimination of platelets against noise and erythrocytes in persons with normal size

distributions of these cell populations. Our microfluidic flow cytometer features integrated hydrodynamic focusing for combined optical and impedance analysis of single cells at high counting rate. The micro flow cytometer was also successfully applied to differentiate WBC in haemolysed blood samples. Lymphocytes, monocytes, neutrophilic and eosinophilic granulocytes can be distinguished by impedance measured at one frequency in combination with side scatter (SSC) of light. Label-free cell identification was validated by applying antibody staining protocols routinely used in conventional flow cytometry. We exploited impedance detection at two frequencies for the differentiation of platelets, erythrocytes and subpopulations of white blood cells in a whole blood sample. Cell concentrations corresponding to the complete blood count (CBC) and the 3-part differential WBC are obtained from AC impedance measurements alone or in combination with side scatter analysis. The sample preparation is reduced to a dilution only.

Materials and methods

Microdevice – design and fabrication

The µFCM (micro flow cytometer) sensor shown in Figure 1 was designed at PTB and custom manufactured by Micronit Microfluidics BV (Enschede, The Netherlands). The microdevice, described in detail in [42], consists of three layers made of two borofloat glass wafers separated by a 14 µm thick dry-film photoresist (TMMF epoxy laminate). All fluidic and electrical connections are located at the top wafer of the chip allowing convenient handling of the micro device. Since the electrodes were deposited on both glass wafers, a silver epoxy was applied to access the upper electrodes from the top. The outer dimensions of the µFCM are 14 mm × 15 mm with a thickness of 2.2 mm. The channel depths are defined by the two-step wet etching process (100 µm and 30 µm) for the glass wafers and the height of the laminate. Etching resulted in rounded edges and oval cross-sections of the glass channels. Sections defined by the laminate only, have a rectangular cross -section. The sample inlet consists of two parts. The first part in flow direction is etched to a channel height of 74 µm and a width of 330 µm. This rectangular channel leads to the second part, where the 330 µm width is reduced by a non-etched funnel to 40 µm. The height is reduced in a single step to 14 µm, defined by a thin laminate of corresponding height. Hence, at the beginning of the tapered section of 1000 µm length the cross section is 300 µm x 14 µm. At the position where the sample suspension is injected into the sheath flow focusing region the cross section amounts to 40 µm x 14 µm. The etched focussing region is followed by the 250 µm long non-etched detection channel with a cross-section of 20 µm x 14 µm (see Figure 1). The length of the Pt electrodes along the flow direction is 20 µm resulting in an impedance detection volume of 20 µm x 14 µm x 20 µm. The distance between the two pairs of electrodes amounts to 30 µm.

When investigating microparticles, haemolysed or non-haemolysed fresh blood samples count rates were about 500 Hz to 1 kHz. The microdevice was in operation for several hours without any issues with respect to blockage. The channel size of our microfluidic structure was designed to avoid clogging by single cells when analysing fresh blood samples. The largest cells in peripheral blood are granulocytes and monocytes. Recently, Niemiec et al. [46] measured the diameter and volume of neutrophils in suspension and obtained 8.85 µm ± 0.44 µm and 363 μm^3. Relative volumes of neutrophils and monocytes for healthy individuals were compared by Suresh et al. [47]. Monocytes were found to be about 18 % larger in volume, corresponding to a volume of 428 μm^3 and a diameter of about 9.4 µm of a volume equivalent sphere. Furthermore, because of the hydrodynamic focusing and due to the elasticity of cells their diameter perpendicular to the direction of flow is further reduced. It should be noted that

in our experience clogging in conventional as well as microflow cytometers is mainly caused by non-reversible agglomeration of cells or of cell fragments, e.g. membranes of RBC in haemolysed blood samples or degraded cells in stored samples. In addition, swelling due to changes in osmotic pressure could result in blocking of small channels. In our experiments, blood samples were analysed within 6h after drawing blood and preparation was adapted to avoid changes of cell size and formation of agglomerates. Furthermore, the funnel shaped region of the sample inlet channel acts as particle filter, which retains agglomerates larger than 14 µm. Because of the relative large volume of this 1000 µm long section, even for samples with higher concentrations of agglomerates the measurements are not hampered.

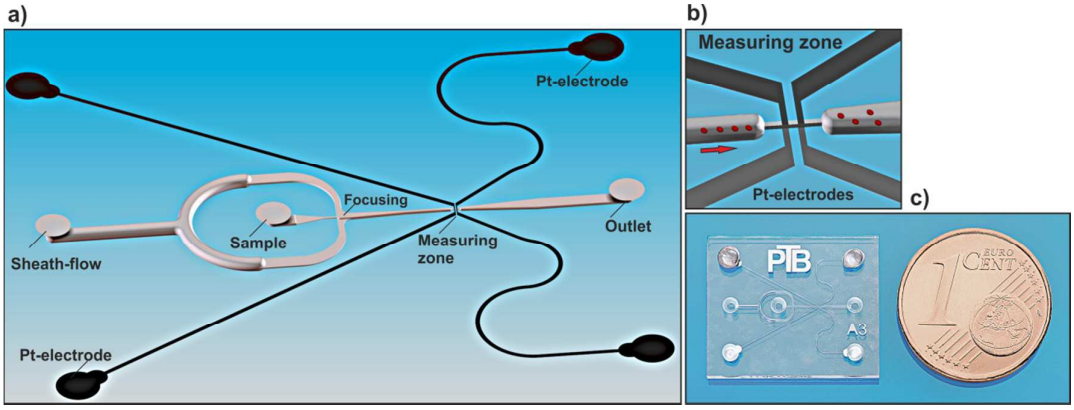

Figure 1: (a) Design of the flow channels and electrodes of the µFCM. **(b)** Close-up of the measuring zone. **(c)** Photo of the µFCM device showing proportions.

Measurement setup and data analysis

The µFCM was mounted on an inverted microscope (Axiovert 35M, Carl Zeiss, Germany). A Fluidic Connect Pro adapter (Micronit Microfluidics, Netherlands) provided connections to the external instrumentation and the fluid handling system. Isotonic solution (ISOTON® II, Beckman Coulter GmbH, Germany) with a conductivity of 1.6 S m^{-1} was used as a sheath fluid in all microparticle and blood measurements. The average pressure of the fluid system was set to 1 bar resulting in volumetric sheath flow rates of 26 µL min^{-1}. A schematic of the setup is shown in Figure 2. The fluid handling system and the optical detection setup were described in detail previously [43], [48]. The sample was injected by a vertically mounted syringe pump (model 540060, TSE Systems GmbH, Germany) with the sample flow rate set between 5 µL min^{-1} and 7 µL min^{-1}. Taking into account the total volume flow rates of the sheath and sample flows particle velocities of about 3.8 m s^{-1} were reached.

The excitation laser beam (continuous wave laser, wavelength 488 nm, Sapphire 488-200, Coherent, USA) was shaped by telescopes to obtain a circular cross-section before entering the microscope objective. Finally, the laser beam is focussed to a diameter of 7 µm measured at full width at half maximum (FWHM). The output power was set to 20 mW. Particles crossed the laser beam 40 µm downstream with respect to the electrode pairs. Light side scatter (SSC) was collected with a multi-mode, 600 µm core diameter optical fibre with a numerical aperture of NA = 0.37 (Laser Components GmbH, Germany). The fibre was positioned at the bottom of the microchip and aligned relatively to the excitation spot. Fluorescence and SSC signals were detected by photomultiplier tubes (PMTs) with appropriate band pass filters.

We used a multi-frequency dual-phase lock-in amplifier system (UHFLI, Zurich Instruments, Switzerland) for detection of the impedance change caused by particles passing the electrode pairs. The UHFLI frequency synthesizer outputs served to apply signal amplitudes of 750 mV for single-frequency measurements and 370 mV per frequency for two-frequency measurements. The current for each electrode pair was amplified with a trans-impedance high speed current amplifier (DHPCA-100, Femto GmbH, Germany). The output voltage signals were subsequently differentiated (DA1855A, Teledyne LeCroy, USA) and analyzed by the UHFLI-demodulator. Up to four UHFLI analog outputs with a digital-to-analog sampling rate of 25 MSamples s^{-1} were used for the measurement of in-phase and out-of-phase impedance components. Analog signals were amplified within a suitably chosen bandpass by low-noise voltage pre-amplifiers (SR560, Stanford Research Systems, USA).

The analog signals derived from optical and impedance measurements were registered using the data acquisition module of a conventional commercial flow cytometer (CyFlow Cube 8 flow cytometer, Partec GmbH, Germany). The pulse heights of the signals were simultaneously detected and digitized with 16-bit resolution using the impedance signal as a trigger. The analog signals from the UHFLI lock-in amplifier were acquired without further processing allowing real-time monitoring and adjustment of the experiment.

For quantitative measurements of cell concentrations counting loss due to random coincidences has to be taken into account. To estimate the counting loss we use the approximation derived in [49]

$$N \approx N_r \frac{1}{1-(N_r \tau/t)} \qquad (1)$$

to calculate the conventional quantity value for the number of events N (i.e. the "true" number of cells) from the number of observed events N_r. The total interaction time τ = 18.4 µs of one

cell passing both electrode pairs follows from the corresponding length of 70 µm and the particle velocity of 3.8 m s^{-1}. In our experiments at a typical count rate of 1 kHz the ratio N_r / N of the recorded number of events and the true particle number amounts to 0.9816 and the corresponding counting loss is 1.84%. Typical numbers for impedance based counters used in haematology are in the order of 10%. For the determination of reference values sequential dilutions are prepared to derive the coincidence corrected cell counts. In such experiments counting losses range between 2% and 10% [50]. It follows that for our applications higher count rates up to 5kHz and a corresponding correction of counting loss of about 10% are reasonable.

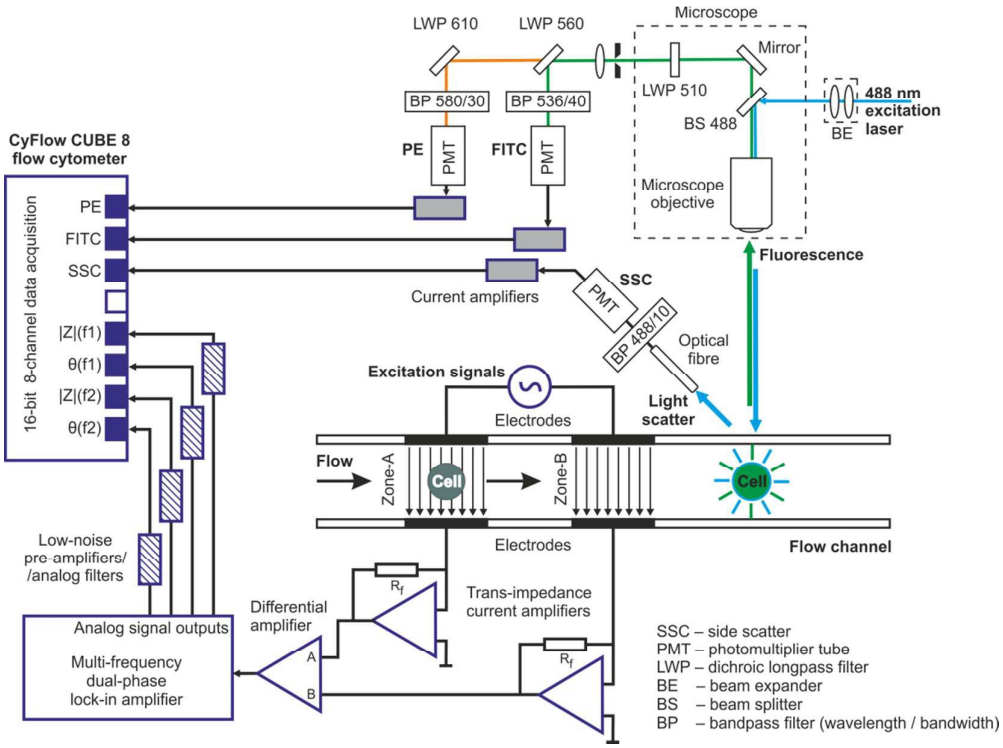

Figure 2: Measurement setup for combined flow cytometric optical and vector impedance measurements of blood cells and microparticles.

Monodisperse fluorescent calibration microparticles

Sensitivity and size resolution of the µFCM were evaluated by the measurement of monodisperse calibration microparticles with different diameters and graded fluorescence intensities. This particle suspension allows to identify particle populations according to their defined size and their specific fluorescence intensity. We prepared a suspension of custom manufactured polystyrene beads with diameters of (2.16±0.03) µm, (3.20±0.13) µm, (4.89±0.08) µm, (6.32±0.11) µm and (8.13±0.12) µm (PS-FluoGreen, Microparticles GmbH, Germany). The particles stained with different amounts of Fluorescent Green dye were measured in the detection channel usually chosen for the observation of the fluorescence of fluorescein isotiocyanat (FITC). With increasing particle diameter, the corresponding total fluorescence intensities varied from 600 MEFL to 85,000 MEFL units (molecules of equivalent soluble fluorescein [51]). The particles were diluted in ISOTON® II (Beckman Coulter, Inc.,

Germany). Low concentrations of about 10^2 beads per µL were prepared to prevent coincidences during measurement.

Human peripheral blood samples

All blood samples were drawn from healthy volunteers who have given their informed consent in written form that the samples were used for research purposes. Fresh venous blood was collected into 2.7 mL tubes (Monovette EDTA K, Sarstedt AG & Co., Germany) containing EDTA as anticoagulant. Concentrations of blood cells were determined using the haematology cell counter ABX Micro ES 60 (Horiba ABX, France) for each sample prior to further processing. To evaluate the performance of the µFCM, we carried out comparison experiments and analysed the same samples with a bench-top cytometer (CyFlow Space, Sysmex Partec GmbH, Germany).

Protocol A was applied to identify leukocyte subpopulations in haemolysed blood samples and to demonstrate the potential of label-free cell discrimination. In addition, the protocol was used to measure the frequency dependence of impedance signals of leukocyte subpopulations. To increase leukocyte concentration 6 mL whole blood were centrifuged with 300 g for 10 min. 700 µL of plasma and 700 µL of sedimented erythrocytes were carefully removed. In that way the leukocyte concentration was increased by about a factor of 2 with respect to erythrocytes avoiding the reduction of relative concentration of granulocytes. For immunologically based cell identification by observation of fluorescence signals CD 45-FITC (BD Pharmingen; CD – Cluster of Differentiation) antibody staining was applied. 20 µL of CD 45-FITC was added to 100 µL of the blood samples containing enriched leukocyte concentrations and incubated for 15 min at room temperature. Subsequently, for haemolysis (CyLyse, Sysmex Partec GmbH) 100 µL of the blood sample was added to 100 µL of the fixation-reagent and incubated for 10 min. Further addition of 2.5 mL lysis-reagent and additional incubation for 20 min resulted in a dilution of 1:27. The concentration of leukocytes amounted to 485 cell μL^{-1}.

Protocol B was used to measure the impedance signals of blood platelets and erythrocytes for frequencies between 300 kHz and 100 MHz. Simultaneously to impedance measurements optical identification by means of staining was performed. Therefore 100 µL whole blood aliquot was added to 200 µL of ISOTON® II and 20 µL of CD 61-PE antibody staining reagent (BD Pharmingen). The stained blood aliquot was incubated for 15 minutes at room temperature. Next, 6.5 µL were removed, mixed with 3 mL of ISOTON® II, and 3 µL of CD 235a-FITC (BD Pharmingen) was added for identification of erythrocytes, resulting in a total dilution of approximately 1:1500 with a concentration of $3.5x10^3$ cells μL^{-1}. Again, the sample was incubated according to the instructions of the manufacturer for additional 15 min at room temperature before measurement.

Protocol C was applied to investigate label-free identification of blood platelets, erythrocytes, granulocytes, monocytes and lymphocytes in whole blood in a single measurement. As described in protocol A, for the reduction of the measurement time the leukocyte concentration was increased by a factor of 2 employing centrifugation and removing erythrocytes and plasma. To validate the differentiation of all leukocyte subpopulations, 100 µL aliquot of whole blood was stained with 20 µL of CD 45-PE (BD Pharmingen) and incubated for 15 min at room temperature. Next, the volume of 50 µL was removed, added to 1100 µL of ISOTON® II and stained with 20 µL of CD 61-FITC (BD Pharmingen) to label platelets. The sample was incubated for additional 15 min and then diluted with ISOTON® II to the total volume fraction of about 1:750 resulting in a concentration of $5.9x10^3$ cells μL^{-1}.

Protocol D includes the minimal preparation required to analyse the populations of platelets, erythrocytes and the three subpopulations of leukocytes in whole blood samples. The unprocessed whole blood sample was diluted with ISOTON® II to the total volume fraction of about 1:350 resulting in a concentration of $14.7x10^3$ cells μL^{-1}.

Characterization of the microdevice

Microparticles: For impedance analysis particles are passing the interaction zones (cf. Figure 2) of both electrode arrays in single file. Differential measurement of the medium with and without the particle between each electrode pair leads to the characteristic dispersion-like signals [34], [42]. Only the pulse height of the negative peak was recorded, since our data acquisition board requires an input of a negative polarity. To determine the limit of detection and the pulse height resolution of the microdevice [52], monodisperse fluorescent particles with diameters ranging from 2.16 µm to 8.13 µm (i.e. volumes of about 5 μm^3 and 280 μm^3) were analysed. The range of the particle size was chosen to correspond to the volumes of the targeted cell populations. Fluorescence and impedance signals were measured simultaneously using the impedance magnitude ($|Z_1|$ at 2.3 MHz) signal as trigger. The histogram shown in Figure 3 was derived from the corresponding two dimensional data set by (colour) gating the different particle populations. The histogram depicts the normalized in-phase amplitudes (real component of Z_1 impedance) for a suspension containing 5 particle populations, the diameters of which are indicated in the figure. To facilitate the comparison of the various distributions, the maximum count for each population was normalized to 100. A linear dependence of the in-phase amplitude and the particle size was observed. Using the known particle diameter for calibration, the upper axis directly reflects the particle volume in fL. The width of the distribution was determined for each particle volume and used as indicator for the pulse height resolution of the impedance measurement. The corresponding coefficients of variation for larger diameter particles are $CV_{8.13\ \mu m}$ = 2.7 % and $CV_{6.32\ \mu m}$ = 4.3 %. CVs measured for smaller particles amount to $CV_{4.89\ \mu m}$ = 7.8 %, $CV_{3.2\ \mu m}$ = 19.8 % and $CV_{2.16\ \mu m}$ = 20.8 %. It should be noted that the width of the distributions for the two largest particle populations are narrower by the factors of 1.6 and 1.2 compared to the manufacturers' specifications. For the smaller particles, however, the CVs exceed the specified values by the factors of 1.5, 1.6 and 5, respectively. The limit of detection (LOD) for the particle volume was estimated from Figure 3 and amounts to about 2 fL for simple real-time threshold based analysis. This approach requires signal-to-noise ratios higher than 1:1. Berkel et al. [26] achieved a LOD of 0.6 fL for larger sensing volumes using pulse shape analysis instead of simple threshold detection. Because of the known shape of the dispersion like signals, even particles with corresponding threshold derived signal-to-noise ratios below 1:1 were analysed. Implementation of such signal processing approach into our data acquisition setup could further improve the LOD. However, taking into account the mean platelet volume ranging from about 7 fL to 12 fL and the corresponding platelet distribution widths of 9 fL to 14 fL, determined at 20% of the height of the volume distribution of platelets, the sensitivity of 2 fL is adequate for the measurement of platelet volume distributions in healthy normal individuals.

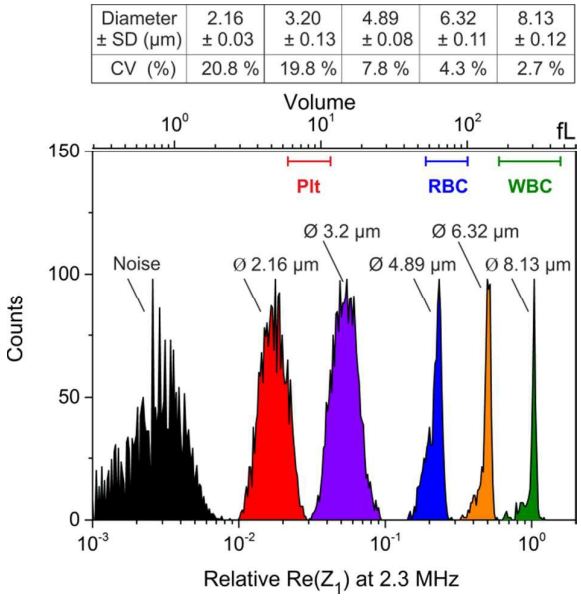

Figure 3: Normalized histogram (in-phase signal amplitudes) of monodisperse fluorescent calibration particles and corresponding coefficients of variations (CV) measured with the µFCM at a frequency of 2.3 MHz. Fluorescence was detected in the FITC channel and applied for colour gating of the particles. The suspension contained custom manufactured polystyrene beads (PS-FluoGreen, Microparticles GmbH, Germany). The driving voltage amplitude was set to its maximum value of 750 mV.

Differentiation of leukocytes in haemolysed blood samples: Differentiation of leukocyte subpopulations based on side and forward light scatter is a commonly used technique in flow cytometry. Small angle forward light scattering can be detected for size based cell differentiation. In addition, orthogonal or side light scatter provides information on the cell structure. Different authors have shown that non-labelled lymphocytes, monocytes and granulocytes can be distinguished by light-scattering measurements [53] [54]. In general, discrimination of leukocyte subpopulations requires haemolysis of erythrocytes which otherwise would obscure leukocyte signals in the side scatter and forward scatter observation channels. Differentiation of leukocyte subpopulations by their electrical properties correlated with cell size and membrane capacity was also reported in literature. Results on leukocyte differentiation using impedance opacity (i.e. ratio of impedance magnitudes measured at high and low frequencies) were shown for a special sample treatment based on haemolysis using formic-acid and saponin [24], [25], [26]. In our previous publication [42] we used two different haemolysis reagents (Cell Kit C05, Cellset AG, Switzerland and CyLyse, Sysmex Partec GmbH, Germany) to evaluate the differentiation of leukocytes. The sample processing did not allow for differentiation of monocytes and granulocytes by impedance measurements alone. CD14-PE fluorescence was applied additionally to discriminate the two subpopulations. Figure 4a shows an alternative approach of the combined optical and electrical differentiation of non-labelled leukocytes in a haemolysed sample measured with the µFCM device. The figure depicts pulse height distributions of the impedance magnitude $|Z_1|$ at 2.3 MHz versus side scatter (SSC) intensity. To validate the label-free differentiation, leukocytes were immunologically stained with CD45-FITC according to protocol A. Identification of targeted leukocyte subpopulations was done according to standard flow cytometric procedure by plotting CD45-FITC fluorescence against SSC intensity at 488 nm wavelength and setting colour gates as shown in the supplement (Figure s1) [42], [48]. The coloured clusters illustrate the four subpopulations of

white blood cells, the lymphocytes (Ly), monocytes (M), neutrophilic granulocytes (G_n) and eosinophilic granulocytes (G_e). Events caused by cell debris and noise are located in the lower left corner. Lymphocytes are clearly separated from cell debris and from granulocytes and monocytes along the $|Z_1|$-parameter axis as seen in Figure 4b, i.e. in the histogram derived from impedance measurement at 2.3 MHz. The effect of overlapping granulocytes and monocytes in impedance measurements was already discussed in our previous publication [42]. We observed that for haemolysed blood samples the analysis of the opacity at 2.3 MHz and 500 kHz does not improve the discrimination between granulocytes and monocytes. The same concerns the frequencies of 10 MHz and 2.3 MHz, which is in contrast to untreated leukocytes as demonstrated in the following section on non-haemolysed blood samples. Therefore side scatter is needed as additional measurand for the reliable differentiation of treated leukocytes. As illustrated in Figure 4a, the four cell subpopulations are easily discernible by combined side scatter and impedance measurement. Absolute cell counts derived from label free and antigen differentiation are in good agreement and differ by 2 % to 3 %, mainly due to uncertainty of applied gating.

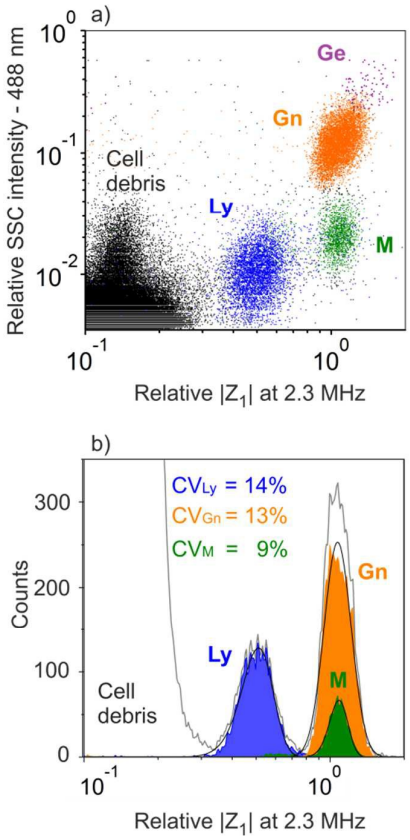

Figure 4: Label-free differentiation of leukocyte subpopulations in the µFCM by combined optical and impedance detection at 2.3 MHz in a haemolysed blood sample. Leukocytes were labelled with anti-CD45-FITC antibodies (protocol A) and colour gated based on the side scatter (SSC) versus CD45-FITC (see supplement) dot plot. **(a)** Distribution of lymphocytes (Ly), monocytes (M), neutrophil granulocytes (G_n) and eosinophil granulocytes (G_e). **(b)** Impedance-histogram and the coefficients of variation (CV) for leukocyte subpopulations. In total 15,000 leukocytes were analyzed. The driving voltage amplitude was set to 370 mV.

Differentiation of platelets and erythrocytes: In microfluidic devices, counting of platelets by non-labelling techniques is challenging due to their small volumes and large size distribution [55]. In particular, in impedance measurements the sensitivity is crucial to avoid loss of platelets of small volumes. The LOD of our µFCM for simple threshold analyses was estimated to be approximately 2 fL by using a suspension of different monodisperse particles (see Figure 3). For persons with typical platelet size distributions this value is sufficiently small to detect all platelets. In Figure 5a, we demonstrate the differentiation of platelets and erythrocytes by measuring the magnitude of impedance at a single frequency of 2.3 MHz versus SSC intensity. The whole blood sample was prepared as described in protocol B and the driving voltage was set to its maximum value of 750 mV. The results of the label-free analysis were validated by the measurement of immunofluorescence of the CD61-PE stained platelets and the CD235a-FITC stained red blood cells (supplement, Figure s2). In Figure 5a, colour gating was applied to the immunolocally identified Plt and RBC populations. The separation of cells is slightly improved by using the SSC intensity as additional information (Figure 5a), but it follows from Figure 5b that label-free differentiation of platelets and erythrocytes is unambiguous based on impedance measurement only. This is consistent with the results previously reported by Berkel et al. [26]. Figure 5b depicts the measurement of an unprocessed whole blood sample according to protocol D including dilution only. No overlapping of populations is evident and platelets are clearly separated from the cell debris and noise. The present setup is not designed for measurement of the absolute cell concentration. However, the difference for absolute cell counts comparing differentiation by the label-free method and by labelling amounts to 3.5 % for platelets and 4 % for erythrocytes (Figure 5a). The comparison of the relative platelet and erythrocyte concentration using the ABX Micro ES 60 haematology cell counter and the microdevice leads to a difference of less than 1 % for the unprocessed whole blood sample (Figure 5b).

We include in the histograms in Figure 4 and Figure 5 the CVs for platelets, erythrocytes and leukocytes (CV_{RBC} = 17 %, CV_{Plt} = 24 %, CV_{Ly} = 14 %, CV_{Gn} = 13%, CV_{M} = 9 %). Compared to microparticles with a similar volume, i.e. with diameters of 2.17 µm, 4.89 µm and 8.12 µm ($CV_{2.17µm}$ = 20.8 %, $CV_{4.89µm}$ = 7.8 % and $CV_{8.12µm}$ = 2.7 %), the CVs observed for cells are much larger. This proves that CVs for cells are dominated by the biological variation and influences due to the instrumental resolution causes minor contributions only. It should be noted that the observed value for RBCs is consistent with the so called red blood cell distribution width (RDW) of 12 % to 14.5 % expected for a normal person.

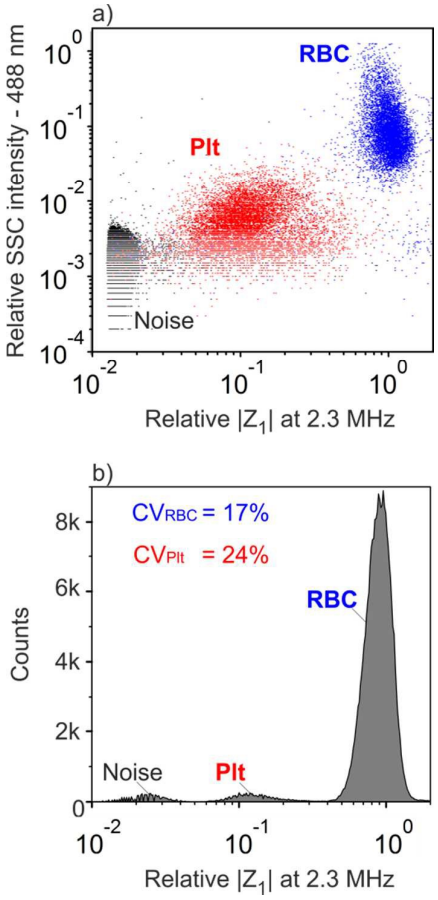

Figure 5: Label-free differentiation of platelets (Plt) and erythrocytes (RBC) in whole blood samples. **(a)** Side scatter (SSC) versus magnitude of impedance $|Z_1|$ at 2.3 MHz. Platelets were labelled with anti-CD61-PE and erythrocytes with anti-CD235a-FITC (protocol B) for verification of the label-free analysis. Colour gating was applied in the PE versus FITC plot (supplement). Approximately 10,000 erythrocytes and 10,000 platelets were measured. **(b)** Cell differentiation by the magnitude of impedance $|Z_1|$ only and the corresponding coefficients of variation (CV) for an unprocessed whole blood sample (protocol D) involving dilution only. Approximately 211,000 erythrocytes and 8,400 platelets were measured. The driving voltage amplitude was set to its maximum value of 750 mV.

Results and discussion

Complete and WBC 3-Part Blood Count in whole blood: The µFCM was applied to differentiate cell populations required for the determination of the Complete Blood Count (CBC) and the three part differential white blood count (WBC 3-Part Blood Count). The sample was prepared according to protocol C which includes dilution to adapt the count rate to the instrumental characteristics. The additional antibody staining step is only necessary for immunological validation of the cell subpopulations. To reduce the measurement time during the optimisation of the µFCM-analysis the concentration of leukocytes was typically increased by a factor of 2. To demonstrate label-free cell differentiation we prepared samples for measurement applying dilution only according to protocol D. In this way potential influences of the applied immunostaining protocol or the leukocyte enrichment procedure were also excluded.

Label-free cell identification by combined optical and impedance measurements is depicted in Figure 6. The results shown in Figure 7 demonstrate the capability of cell differentiation for the CBC and WBC 3-Part Blood Count in whole blood based on impedance measurements alone. The identification of the cell populations in Figures 6 and 7 was validated using the immunofluorence of CD-45 and CD-61 antibodies specific for white blood cells and platelets, respectively. The population of erythrocytes can be identified by correlation with Figure 5. In Figure 6a, the results for a commercial bench-top flow cytometer (FCM) are shown for comparison. The colour assignment was derived from gating in the corresponding fluorescence diagrams. In the side scatter versus forward light scatter (FSC) dot plot it is obvious that WBC and RBC signals coincide and hence differentiation is not possible. The potential of the µFCM with respect to combined optical and impedance based label-free cell differentiation is demonstrated in Figures 6b and 6c, were SSC intensity versus magnitude of impedance signal is depicted. Approximately 500,000 cells including 1500 leukocytes were measured. Impedance signals at frequencies of 2.3 MHz and 10 MHz were simultaneously acquired. A frequency of 2.3 MHz was chosen, because of the maximized sensitivity of the setup at this frequency. Analysing the frequency dependence of the impedance magnitude for various cell types an enhanced differentiation between leukocytes and erythrocytes was observed at about 10 MHz. Due to the voltage output limitation of the lock-in amplifier the AC voltage for each frequency was reduced from 750 mV to 370 mV resulting in a corresponding decrease of the signal-to-noise ratio by a factor of 2 compared to Figure 5. In contrast to the light scatter measurements performed with the FCM (Figure 6a), the data acquired with the µFCM (Figures 6b and 6c) easily allows discrimination of erythrocytes and leukocytes and observation of leukocyte subpopulations. The separation between red blood cells and the subpopulations of leukocytes (Ly, M, G_n) is improved by detecting impedance signals at a frequency of 10 MHz instead of 2.3 MHz, as seen from comparison of Figures 6b and 6c.

We demonstrate the full potential of AC impedance detection to perform the Complete and WBC 3-Part Blood Count in a non-labelled whole blood sample in Figure 7. The diagrams 7a and 7b depict the magnitude of impedance versus the ratio $Im(Z_2)/Re(Z_1)$ of the reactance at 10 MHz (out-of-phase signal) to the resistance (in-phase signal) at 2.3 MHz. The reactance is proportional to the capacitance of the cell membrane and the resistance is proportional to the size of the cell. Therefore the ratio is proportional to the capacitance of the cell per volume unit [8], [9], [56], [57], [58]. Simultaneous detection of these both quantities enables the differentiation of the five targeted cell populations without the need of a laser and optical components. To visualise the performance of the impedance method for leukocyte differentiation in whole blood, the corresponding region of interest is enlarged in Figure 8a. Figure 8b depicts the measurement of an unprocessed whole blood sample according to protocol D including dilution only. The cell populations were identified by comparison with the corresponding clusters in Figure 8a. In contrast to the haemolysed sample (see Figure 4) we are

able to differentiate untreated leukocytes by their electrical properties only, plotting impedance magnitude $|Z_2|$ against $Im(Z_2)/Re(Z_1)$. To check the consistency of our data, we compared absolute cell counts derived from impedance measurements with results obtained from antigen differentiation and combined impedance and side scatter detection. We observed differences of 1 % for granulocytes, 2 % for monocytes and 6 % for lymphocytes with respect to antigen based fluorescence. Using the combined impedance and light scatter experiment the difference for lymphocytes is reduced to about 3% since contributions from large erythrocytes or agglomerates can be removed. Such deviations are significantly smaller compared to variations (20%) observed in interlaboratory surveys, e.g. for CD4 positive cells [59], thus indicating the capability of our µFCM for absolute concentration measurements.

Our results prove the feasibility of the microfluidic device for label-free differentiation of platelets, erythrocytes, granulocytes, monocytes and lymphocytes in a single measurement by impedance analysis alone or combined with optical detection. As stated above, the only necessary sample treatment involves dilution of the whole blood suspension. At present the practical applicability is hampered by the measurement time which was about 45 min for the diluted sample using protocol D and a corresponding count rate of approximately 1 kHz. To eliminate this disadvantage further optimization is needed. Besides the increase in particle velocity by a factor of two as already demonstrated [42], cell concentrations in the measurement suspension can be increased by about a factor of 5. To determine the coincidence corrected number of counts (N) equation (1) shall be applied. Hence, we expect that the measurement time can be reduced to less than 5 min. It follows that the whole blood cell differentiation by AC measurements is suited to replace microscopic evaluation of samples were differentiation of white blood cell subpopulations with high throughput haematology analysers fails.

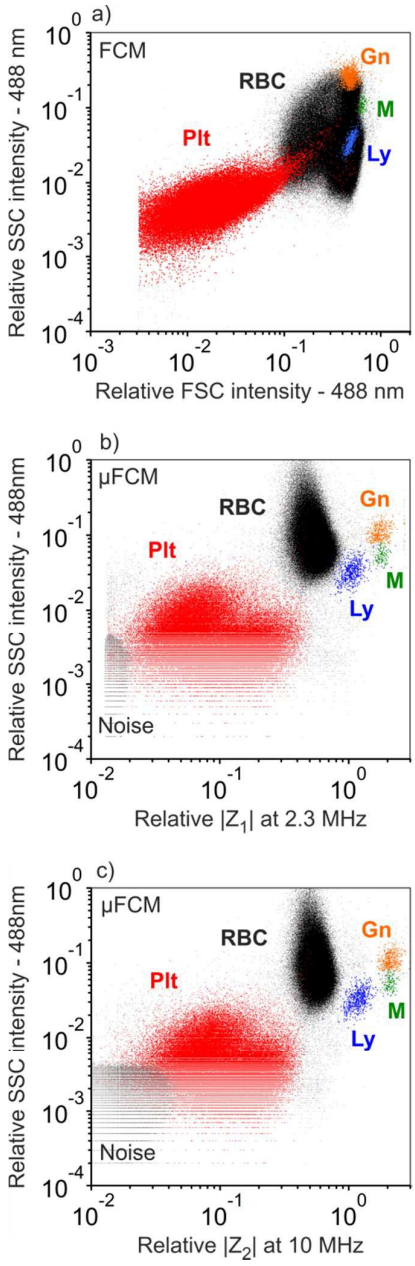

Figure 6: (a) Side scatter (SSC) versus forward scatter (FSC) intensity measured by the CyFlow Space bench-top flow cytometer (FCM). The whole blood sample was prepared according to protocol C. For identification, leukocytes were labelled with anti-CD45-FITC and platelets with anti-CD61-PE. Colour gating was applied in SSC intensity versus FITC fluorescence intensity and FITC fluorescence intensity versus PE fluorescence intensity plots. For clarity, the dots of gated populations are enlarged compared to the non-gated RBC population. **(b, c)** Side scatter (SSC) intensity versus magnitude of impedance at 2.3 MHz and 10 MHz measured with the µFCM for the same whole blood sample. The magnitude of impedance at 10 MHz enables differentiation of erythrocytes and leukocytes. Approximately 500,000 cells (1500 leukocytes) were detected in the µFCM and FCM devices. The measurement time for the µFCM amounted to 25 min and the driving voltage amplitude was set to 370 mV for each frequency.

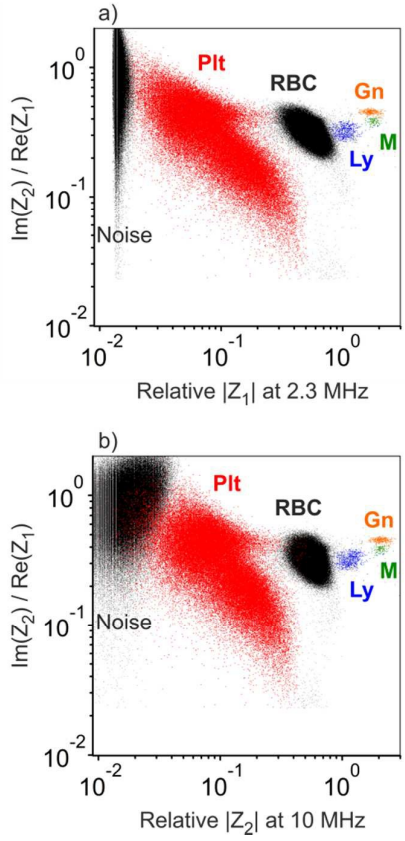

Figure 7: (a, b) Magnitude of impedance versus the ratio ($Im(Z_2)/Re(Z_1)$) of reactance at 10 MHz (out-of-phase signal) to resistance (in-phase signal) at 2.3 MHz in a whole blood sample for the µFCM. Protocol C was applied for preparation of the sample and identification was achieved according to Figure 6. Both plots emphasize the differentiation of platelets (Plt), erythrocytes (RBC), lymphocytes (Ly), monocytes (M) and neutrophil granulocytes (G_n) by their electrical properties only.

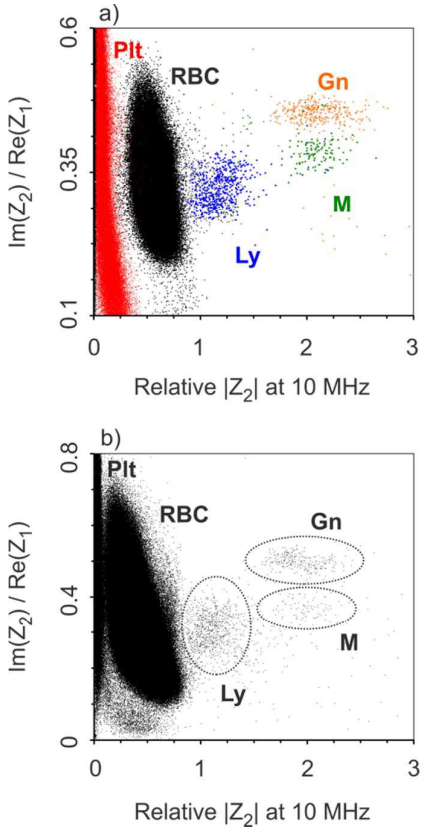

Figure 8: Extended region of scatterplots with linear scaled axes showing differentiation of leukocyte subpopulations. **(a)** The sample was prepared according to protocol C including immunostaining and leukocyte enrichment. Approximately 500,000 cells (1500 leukocytes) were analyzed in 25 min. **(b)** The unprocessed whole blood sample was prepared according to protocol D including dilution only. Approximately 3,000,000 cells (1800 leukocytes) were analyzed in 45 min.

Summary and conclusions

We have developed a microfluidic sensor and demonstrated its applicability for label-free leukocyte differentiation in a whole blood sample by AC impedance measurements. The structure features sheath flow hydrodynamic focusing and a double pair of electrodes. The device facilitates the simultaneous measurement of multi-frequency impedance signals and optical signals. For the validation of the identification of leukocyte subpopulations, the optical detection channels were used to analyse immunofluorescence signals of stained cells. The performance of the microflow cytometer was characterised by monodisperse microparticles in the size range corresponding to the volumes of the targeted cells, i.e. platelets, red blood cells and white blood cells in fresh blood samples. The standard protocol used in haematology analysers, i.e. the measurement of platelets and red blood cells in a diluted sample and white blood cell differentiation in a haemolysed sample was also applied. We proved the capability of our micro chip to differentiate platelets and red blood cells and to determine their relative concentrations by AC impedance measurements. White blood cell differentiation was achieved in haemolysed blood samples by combined AC impedance and light scatter analysis. Hence, the structure was demonstrated to allow cell differentiation for the Complete Blood Count and

WBC 3-Part Blood Count. The results of these experiments served as basis for our investigations of non-haemolysed diluted whole blood samples.

The microflow cytometer investigated enables the differentiation of platelets, erythrocytes, granulocytes, monocytes and lymphocytes in whole blood in a single measurement applying impedance detection only or in combination with light scatter analysis. Apart from the dilution of the fresh blood sample, no additional preparation steps are required to perform the Complete Blood Count and the WBC 3-Part Blood Count. This is advantageous compared to standard label-free protocols demanding measurement of haemolysed samples and whole blood samples separately. Alterations of white blood cell volume, shape and integrity induced by haemolysis are avoided.

Future efforts to improve label-free microfluidic based procedure for practical applications concern the optimisation of the AC frequencies with respect to the differentiation of the white blood cells, the increase of the sample throughput and the analysis of the pulse shape of the AC impedance signals [26] to improve the signal to noise ratio. In addition, systematic investigations of samples from normal persons and material from patients are required. To foster practical use, the dilution step might be directly combined with venipuncture, a technique used when anticoagulants shall be avoided. Potential applications of the µFCM include rapid determination of blood platelet concentration during surgery, the differentiation of white blood cells in whole blood samples of patients with haemolysis-resistant red blood cells, differentiation of haemolysis sensitive white blood cells in leukaemia patients and partial replacement of microscopic evaluation of samples exhibiting non-identifiable cell populations in a high throughput flow cytometer.

Acknowledgements

The work was partly supported by the German Federal Ministry for Economic Affairs and Energy within the funding program ‘Messen, Normen, Prüfen und Qualitätssicherung’ (MNPQ).

The authors would like to thank Rainer Macdonald and Andreas Kummrow for valuable scientific discussions, Alfred Walter for help in setting up the high frequency impedance detection, Uwe Jagemann, Stephan Reitz, Klaus Witt and Robert Häfner for providing technical assistance.

References

[1] H. M. Shapiro, Practical Flow Cytometry, New Jersey: John Wiley & Sons, 2005.

[2] D. A. Ateya, J. S. Erickson, P. B. J. Howell and L. R. Hilliard et al., "The good, the bad, and the tiny: a review of microflow cytometry," *Anal Bioanal Chem,* vol. 391, pp. 1485-1498, 2008.

[3] C. Briggs, "Quality counts: new parameters in blood cell counting," *Int. Jnl. Lab. Hem.,* vol. 31, pp. 277-297, 2009.

[4] W. H. Coulter, "High speed automatic blood cell counter and cell size analyzer," *National Electronics Conference, Inc.,* vol. 12, pp. 1034-1042, 1956.

[5] M. D. Graham, "The Coulter Principle: Foundation of an Industry," *JALA,* vol. 8, pp. 72-81, 2003.

[6] R. A. Thomas, T. A. Yopp, B. D. Watson and D. H. Hindman et al., "Combined optical and electronic analysis of cells with the AMAC transducers," *J Histochem Cytochem,* vol. 25, pp. 827-835, 1977.

[7] R. A. Hoffman and W. B. Britt, "Flow-System Measurement of Cell Impedance Properties," *J Histochem Cytochem,* vol. 27, pp. 234-240, 1979.

[8] S. Gawad, K. Cheung, U. Seger and A. Bertsch et al, "Dielectric spectroscopy in a micromachined flow cytometer: theoretical and practical considerations," *Lab Chip,* vol. 4, pp. 241-251, 2004.

[9] R. A. Hoffman, T. S. Johnson and W. B. Britt, "Flow Cytometric Electronic Direct Current Volume and Radiofrequency Impedance Measurements of Single Cells and Particles," *Cytometry,* vol. 1, pp. 377-384, 1981.

[10] A. M. Cenci, M. Maconi and B. Casolari, "Evaluation of the Diagnostic Performance of the Sysmex XT-2000i Automated Hematology Analyzer in the Detection of Immature Granulocytes," *Sysmex J Int,* vol. 15, pp. 1-6, 2005.

[11] R. Kendall, E. Benoit, J. Bogiages and R. Bordenkircher et al., "Performance evaluation of the Abbott Cell-Dyn 1800 automated hematology analyzer," *Lab Hematol.,* vol. 9, pp. 143-152, 2003.

[12] N. Harris, J. Kunicka and A. Kratz, "The ADVIA 2120 hematology system: flow cytometry-based analysis of blood and body fluids in the routine hematology laboratory," *Lab Hematol.,* vol. 11, pp. 47-61, 2005.

[13] G. Valet, "Past and present concepts in flow cytometry: A European perspective," *J Biol Regul Homeost Agents,* vol. 17, pp. 213-22, 2003.

[14] N. Tatsumi, I. Tsuda, A. Furota and T. Takubo et al., "Principle of Blood Cell Counter- Development of Electric Impedance Method," *Sysmex J Int,* vol. 9, pp. 8-20, 1999.

[15] G. Bourner, J. Dhaliwal and J. Sumner, "Performance evaluation of the latest fully automated hematology analyzers in a large, commercial laboratory setting: a 4-way, side-by-side study," *Lab. Hematol.,* vol. 11, pp. 1-13, 2005.

[16] L. Meintker, J. Ringwald, M. Rauh and S. W. Krause, "Comparison of Automated Differential Blood Cell Counts From Abbott Sapphire, Siemens Advia 120, Beckman Coulter DxH 800, and Sysmex XE-2100 in Normal and Pathologic Samples," *Am J Clin Pathol,* vol. 139, 2013.

[17] N. Tatsumi, I. Tsuda and H. Matsumoto, "Sickle cells show low expansibility and high resistance to saponin," *Folia Haematologica,* vol. 112, pp. 424-435, 1985.

[18] R. Serrani, D. Alonso and J. L. Corchs, "States of stability/lysis in human fetal and adults red blood cells.," *Arch Int Physiol Biochim.,* vol. 97, pp. 309-316, 1989.

[19] V. Ost, J. Neukammer and H. Rinneberg, "Flow Cytometric Differentiation of Erythrocytes and Leukocytes in Dilute Whole Blood by Light Scattering," *Cytometry,* vol. 32, pp. 191-197, 1998.

[20] X. Li, W. Chen, G. Liu and W. Lu et al., "Continuous-flow microfluidic blood cell sorting for unprocessed whole blood using surfacemicromachined microfiltration membranes," *Lab Chip,* vol. 14, p. 2565–2575, 2014.

[21] J. A. Davis, D. W. Inglis, K. J. Morton and D. A. Lawrence et al., "Deterministic hydrodynamics: Taking blood apart," *PNAS,* vol. 103, p. 14779–14784, 2006.

[22] S. Choi, S. Song, C. Choi and J. Park, "Continuous blood cell separation by hydrophoretic filtration," *Lab Chip,* vol. 7, p. 1532–1538, 2007.

[23] M. Yamada and M. Seki, "Hydrodynamic filtration for on-chip particle concentration and classification utilizing microfluidics," *Lab Chip,* vol. 5, p. 1233–1239, 2005.

[24] D. Holmes, D. Pettigrew, C. H. Reccius and H. Morgan, "Leukocyte analysis and differentiation using high speed microfluidic single cell impedance cytometry," *Lab Chip,* vol. 9, pp. 2881-2889, 2009.

[25] D. Spencer, G. Elliot and H. Morgan, "A sheath-less combined optical and impedance micro-cytometer," *Lab Chip,* vol. 14, pp. 3064-6073, 2014.

[26] C. v. Berkel, J. D. Gwyer, S. Deane and N. Green et al., "Integrated systems for rapid point of care (PoC) blood cell analysis," *Lab Chip,* vol. 11, pp. 1249-1255, 2011.

[27] J. Nguyen, Y. Wei, Y. Zheng and C. Wang et al., "On-chip sample preparation for

complete blood count from raw blood," *Lab Chip,* vol. 15, p. 1533–1544, 2015.

[28] S. Gawad, L. Schild and P. Renaud, "Micromachined impedance spectroscopy flow cytometer for cell analysis and particle sizing," *Lab Chip,* vol. 1, pp. 76-82, 2001.

[29] D. Spencer, V. Hollis and H. Morgan, "Microfluidic impedance cytometry of tumour cells in blood," *Biomicrofluidics,* vol. 8, 2014.

[30] S. Crocetti, C. Beyer, G. Schade and M. Egli et al., "Low Intensity and Frequency Pulsed Electromagnetic Fields Selectively Impair Breast Cancer Cell Viability," *PLOS ONE,* vol. 8, pp. 1-13, 2013.

[31] S. Crocetti, C. Beyer, S. Unternährer and T. B. Damm et al., "Impedance Flow Cytometry Gauges Proliferative Capacity by Detecting TRPC1 Expression," *Cytometry Part A,* vol. 85A, pp. 525-536, 2014.

[32] A. Pierzchalski, M. Hebeisen, A. Mittag and J. Bocsi et al., "Label-free hybridoma cell culture quality control by a chip-based impedance flow cytometer," *Lab Chip,* vol. 12, pp. 4533-4543, 2012.

[33] J. Chen, C. Xue, Y. Zhao and D. Chen et al., "Microfluidic Impedance Flow Cytometry Enabling High-Throughput Single-Cell Electrical Property Characterization," *Int. J. Mol. Sci.,* vol. 16, pp. 9804-9830, 2015.

[34] T. Sun and H. Morgan, "Single-cell microfluidic impedance cytometry: a review," *Microfluid Nanofluid,* vol. 8, pp. 423-443, 2010.

[35] K. C. Cheung, M. D. Berardino, G. Schade-Kampmann and M. Hebeisen et al., "Microfluidic Impedance-Based Flow Cytometry," *Cytometry part A,* vol. 77A, pp. 648-666, 2010.

[36] Y. Zheng, J. Nguyen, Y. Wei and Y. Sun, "Recent advances in microfluidic techniques for single-cell biophysical characterization," *Lab Chip,* vol. 13, pp. 2464-2483, 2013.

[37] H. Morgan and D. Spencer, "Microfluidic Impedance Cytometry for Blood Cell Analysis," in *Microfluidics for Medical Applications*, The Royal Society of Chemistry, 2015, pp. 213-241.

[38] A. van den Berg and L. Segerink, Microfluidics for Medical Applications, Cambridge: The Royal Society of Chemistry, 2015.

[39] I. Cheng, H. Chang, D. Hou and H. Chang, "An integrated dielectrophoretic chip for continuous bioparticle filtering, focusing, sorting, trapping, and detecting," *Biomicrofluidics,* vol. 1, pp. 021503:1-15, 2007.

[40] T. Laurell, F. Petersson and A. Nilsson, "Chip integrated strategies for acoustic separation and manipulation of cells and particles," *Chem. Soc. Rev.,* vol. 36, p. 492–506, 2007.

[41] M. E. Piyasena, P. P. A. Suthanthiraraj, R. W. J. Applegate and A. M. Goumas et al, "Multinode Acoustic Focusing for Parallel Flow Cytometry," *Anal. Chem.,* vol. 84, pp. 1831-1839, 2012.

[42] M. Frankowski, P. Simon, N. Bock and A. El-Hasni et al., "Simultaneous optical and impedance analysis of single cells: A comparison of two microfluidic sensors with sheath flow focusing," *Eng. Life Sci.,* vol. 15, pp. 286-296, 2015.

[43] M. Frankowski, J. Theisen, A. Kummrow and P. Simon et al., "Microflow Cytometers with Integrated Hydrodynamic Focusing," *Sensors,* vol. 13, pp. 4674-4693, 2013.

[44] A. Kummrow, J. Theisen, M. Frankowski and A. Tuchscheerer et al., "Microfluidic structures for flow cytometric analysis of hydrodynamically focussed blood cells fabricated by ultraprecision micromachining," *Lab Chip,* vol. 9, pp. 972-981, 2009.

[45] X. Xuan, J. Zhu and C. Church, "Particle focusing in microfluidic devices," *Microfluid Nanofluid,* vol. 9, pp. 1-16, 2010.

[46] M. J. Niemiec, B. D. Samber, J. Garrevoet and E. Vergucht et al., "Trace element landscape of resting and activated human neutrophils on the sub-micrometer level," *Metallomics,* vol. 7, pp. 996--1010, 2015.

[47] P. K. Suresh, J. Minal, P. S. Rao and K. Ballal et al., "Volume Conductivity and Scatter Parameters as an Indicator of Acute Bacterial Infections by the Automated Haematology Analyser," *Journal of Clinical and Diagnostic Research,* vol. 10, pp. EC01-EC03, 2016.

[48] M. Frankowski, N. Bock, A. Kummrow and S. Schädel-Ebner et al., "A Microflow Cytometer Exploited for the Immunological Differentiation of Leukocytes," *Cytometry Part A,* vol. 79A, pp. 613-624, 2011.

[49] M. Kammel, A. Kummrow and J. Neukammer, "Reference measurement procedures for the accurate determination of cell concentrations: present status and future developments," *J Lab Med,* vol. 36, pp. 25-35, 2012.

[50] S. M. Lewis, J. M. England and F. Kubota, "Coincidence correction in red blood cell counting," *Phys. Med. Biol.,* vol. 34, pp. 1159-1162, 1989.

[51] A. Schwartz, L. Wang, G. E. Marti and E. Early et al., "Quantitating Fluorescence Intensity from Fluorophore: The Definition of MESF Assignment," *J. Res. Natl. Inst. Stand. Technol.,* vol. 107, pp. 83-91, 2002.

[52] R. A. Hoffman and J. C. S. Wood, "Characterization of Flow Cytometer Instrument Sensitivity," *Cytometry Protocols,* no. DOI: 10.1002/0471142956.cy0120s40, 2007.

[53] L. W. M. M. Terstappen, B. G. de Grooth, K. Visscher and F. A. v. Kouterik, "Four-Parameter White Blood Cell Differential Counting Based on Light Scattering Measurements," *Cytometry,* vol. 9, pp. 39-43, 1988.

[54] G. C. Salzman, J. M. Crowell, J. C. Martin and T. T. Trujillo et al., "Cell classification by laser light scattering: identification and separation of unstained leukocytes," *Acta Cytol.,* vol. 19, pp. 374-377, 1975.

[55] M. Evander, A. J. Ricco, J. Morser and G. T. Kovacs, "Microfluidic impedance cytometer for platelet analysis," *Lab Chip,* vol. 13, pp. 722-729, 2013.

[56] D. M. Vykoukal, P. R. C. Gascoyne and J. Vykoukal, "Dielectric characterization of complete mononuclear and polymorphonuclear blood cell subpopulations for label-free discrimination," *Integr. Biol.,* vol. 1, pp. 477-484, 2009.

[57] S. Dharia, H. E. Ayliffe and R. D. Rabbitt, "Single cell electric impedance topography: Mapping membrane capacitance," *Lab Chip,* vol. 9, pp. 3370-3377, 2009.

[58] H. Morgan, T. Sun, D. Holmes and N. G. Green et al., "Single cell dielectric spectroscopy," *J. Phys. D: Appl. Phys.,* vol. 40, pp. 61-70, 2007.

[59] R. Stebbings, L. Wang, J. Sutherland and M. Kammel, "Quantification of cells with specific phenotypes I: Determination of CD41 cell count per microliter in reconstituted lyophilized human PBMC prelabeled with anti-CD4 FITC antibody," *Cytometry Part A,* vol. 87, pp. 244-253, 2015.